

available at www.sciencedirect.comjournal homepage: www.elsevier.com/locate/aca

Numerical optimization of matrix-assisted laser desorption/ionization time-of-flight mass spectrometry: Application to synthetic polymer molecular mass distribution measurement[☆]

W.E. Wallace^{*}, C.M. Guttman, K.M. Flynn, A.J. Kearsley

National Institute of Standards and Technology, 100 Bureau Drive, Stop 8541, Gaithersburg, MD 20899-8541 USA

ARTICLE INFO

Article history:

Received 21 February 2007

Received in revised form

23 April 2007

Accepted 22 May 2007

Published on line 26 May 2007

Keywords:

Implicit filtering

Instrument optimization

Objective function

Standards

Stochastic gradient approximation

ABSTRACT

A novel approach is described for the selection of optimal instrument parameters that yield a mass spectrum which best replicates the molecular mass distribution of a synthetic polymer. The application of implicit filtering algorithms is shown to be a viable method to find the best instrument settings while simultaneously minimizing the total number of experiments that need to be performed. This includes considerations of when to halt the iterative optimization process at a point when statistically-significant gains can no longer be expected. An algorithm to determine the confidence intervals for each parameter is also given. Details on sample preparation and data analysis that ensure stability of the measurement over the time scale of the optimization experiments are provided. This work represents part of an effort to develop an absolute molecular mass distribution polymer Standard Reference Material.

Published by Elsevier B.V.

1. Introduction

There has been sustained interest in the use of matrix-assisted laser desorption/ionization (MALDI) mass spectrometry as a means to measure quantitatively the molecular mass distribution (MMD) of synthetic polymers ever since Tanaka et al. [1] first demonstrated the technique on poly (ethylene glycol) and poly (propylene glycol) almost 20 years ago. As early as the second paper in the field in 1992 Wilkins and coworkers [2] pointed out the importance of the proper choice of ion-extraction delay time following the laser ablation event and its possible role in mass discrimination. In the same year

Hillenkamp and coworkers [3] investigated the mass discrimination that arises from the loss of detector sensitivity for higher mass oligomers, which often results in an underestimation of the moments of the polymer MMD. From that time forward the central role of instrument tuning on the accurate determination of the MMD has been a widely recognized. McEwen et al. [4] in the context of wide-polydispersity polymers were the first to examine systematically the specific role of instrumentation in the measurement of the MMD. They concluded that instrumental effects play as significant a role as do laser desorption/ionization effects. In 1999 Vitalini et al. [5] explored the interplay between ion-extraction delay time

[☆] Official contribution of the National Institute of Standards and Technology; not subject to copyright in the United States.

^{*} Corresponding author. Tel.: +1 301 975 5886; fax: +1 301 975 3928.

E-mail address: William.Wallace@nist.gov (W.E. Wallace).

URL: <http://www.nist.gov/maldi> (W.E. Wallace).

and ion-extraction voltage on the measured peak resolution and mass accuracy of mixtures of poly (ethylene glycols). They discovered that highest resolution and mass accuracy could not be obtained across all parts of a wide-polydispersity polymer, only parts of the spectrum could be optimized for any given machine settings. Vitalini et al. conducted their experiment by systematically varying each of the two instrument parameters to map out in full the two-dimensional parameter space. This necessitated taking hundreds of spectra. If they had added a third parameter and sought the same coverage of the parameter space their effort would easily have expanded into thousands of spectra. Beyond three parameters the experiments necessary would have become prohibitively time consuming. To reduce the number of experiments that need to be performed when studying the effects of more than two parameters, Wetzel et al. [6] used an orthogonal experimental design to isolate the effects of five instrument parameters (and two sample parameters) on the signal-to-noise ratio of polystyrene MALDI mass spectra. The use of an orthogonal experimental design allowed for a large number of parameters to be studied but did not require complete coverage of the parameter space. While the work of Wetzel et al. revealed which parameters played the greatest role in determining signal-to-noise ratio it did not explicitly provide a means to optimize that ratio.

A variety of mathematical methods exist that allow the experimentalist to optimize instrument settings without performing an exhaustive search of the parameter space. Broadly classified, these methods are all forms of *numerical optimization*. When the topology of the search space is very complex, for example when it has great sensitivity to one or more parameters (as mass spectrometers often do), the methods used are part of the field of *non-linear programming* [7]. They are called non-linear because some (or all) of the instrument parameters do not have a linear relationship between parameter value and measurement response, that is, the derivative of the parameter-value versus measurement-response curve is not a constant. A simple example is laser intensity and its effect on signal-to-noise ratio where a relatively sharp threshold is observed experimentally. When the measurement outcomes (which in the present case are mass spectra) contain random noise the mathematical methods are termed *stochastic numerical optimization* [8,9]. Stochastic methods are important in mass spectrometry because all mass spectra have noise, this noise varies as the instrument parameters are adjusted, and the noise will often change across the spectrum. In this case, we will use the word noise to mean uncorrelated, random variations in the spectrum as a function of instrument parameters. Measurement noise presents a significant challenge to any optimization method especially for cases where signal-to-noise is not the measurand to be optimized. Nevertheless, numerical optimization methods offer experimentalists a way to tune the instrument parameters to achieve the desired goal without having to search all possible parameter combinations.

A type of numerical optimization known as *genetic search* has been applied recently by Kell and coworkers [10] to the optimization of electrospray ionization (ESI) mass spectrometry in the study of proteins. They optimized 14 instrument settings to achieve the highest simultaneous detection effi-

ciency for five proteins in an equimolar mixture. They found that the optimal settings for any one protein are not the optimal settings for the mixture of proteins. Furthermore, some instrument settings have several optimal (or near-optimal settings) while others show an unambiguous single optimal value. In a more recent paper Kell and coworkers [11] have gone on to show how genetic algorithms can be used to automatically (that is, without operator intervention) optimize a gas-chromatography-mass spectrometer (GC-MS) over nine instrument variables. Using mass spectrometry and working to identify the various metabolites in human serum and yeast fermentations they define a multiobjective optimization function where not only the signal-to-noise ratio but also the total number of peaks and the total run time of the chromatographic separation were optimized simultaneously.

To measure the absolute molecular mass distribution of a synthetic polymer, it would be ideal to locate a region in parameter space where the instrument response function was uniform across the entire mass range. Finding the instrument response function is necessary to calibrate the intensity axis of the mass spectrum, that is, to go from mass spectrum to molecular mass distribution. If the instrument response function is uniform then the relative peak areas in the mass spectrum correspond directly to the relative abundances of individual *n*-mers in the sample. A uniform instrument response function would be a line of zero slope, that is, it would have a derivative of zero. If not uniform, the instrument response function could slowly vary across the mass range, preferably linearly with mass. The optimal conditions are those that give the simplest (or flattest) instrument response function, that is, the one with the smallest derivative.

To determine the instrument response function, a gravimetric mixture was made consisting of three low-polydispersity polystyrenes that were very close in average molecular mass. The optimal instrument settings were those that provided the closest match between the total integrated peak intensity of each of the three polymers in the mass spectrum with the known gravimetric ratios. Note that there is no guarantee (or even assumption) that the optimal instrument settings that give the flattest instrument response function will also yield optimal signal-to-noise ratios. In fact there is no reason to believe that a search for the instrument settings that optimize the gravimetric ratios will not lead into a region where the mass spectra become so noisy as to make peak integration impossible. Thus, to find the optimal instrument settings we used *stochastic gradient approximation methods* [8,9]. These methods have proven to be extremely robust in cases where the measured data are very noisy.

2. Experimental methods

2.1. Polymer samples

Instrument optimization was performed using a gravimetric mixture of three polystyrene samples custom synthesized by Scientific Polymer Products, Inc. (Ontario, NY) [12]. The samples were made by anionic polymerization using either *n*-butyl lithium or *n*-octyl lithium as initiators. Each was terminated with a proton. Their molecular mass distributions were

measured by the vendor using gel permeation chromatography (GPC) with light scattering detection. By this method the two *n*-octyl polystyrenes had number-average molecular masses (M_n) of 6100 u and 12160 u, and the *n*-butyl polystyrene had an M_n of 9030 u. Each had a polydispersity of 1.01 or less. The initiation of two samples with *n*-octyl lithium was employed to allow separation of overlapping molecular mass distributions in the mass spectrum. The as-received samples were heated in a vacuum oven at 60 °C for 24 h to remove any residual solvent. This was important since the method is based on knowing accurate gravimetric ratios between the polymers.

2.2. Reagents

The MALDI matrix used was all-*trans* retinoic acid (RA) purchased from Aldrich Chemical (Milwaukee, WI) and used without purification. The retinoic acid was stored in a freezer. Silver trifluoroacetate (AgTFA) (Aldrich) was the cationizing agent and was used as received. The solvent was unstabilized tetrahydrofuran (THF) (Aldrich). The THF was checked before each experiment for presence of peroxides using Quantofix Peroxide 100 test strips (Macherey-Nagel, Düren, Germany).

2.3. Mass spectrometry

The experiments were performed on a BrukerDaltonics (Billerica, MA) Reflex II MALDI-TOF mass spectrometer in reflectron mode using a dual microchannel plate detector. A nitrogen gas laser (337 nm photon wavelength) with a 3 ns pulse width was used. The laser intensity was varied using a continuously-variable neutral density filter. The sample plate was held at 25 000 V. An extraction plate approximately 2 mm from the sample plate initially held at sample-plate voltage but subsequently pulsed to a lower voltage was used to pull the ions out of the ablation plume. The extraction-plate voltage drop and the delay time for the extraction pulse were variable. The delay time could be varied in three steps of 250 ns, 500 ns, and 750 ns corresponding to 'short', 'medium', and 'long' extract times. The instrument used a variable-voltage Einzel lens to focus the ions into the reflectron whose backing plate voltage was held at 26 250 V. Lastly, the voltage applied to the dual microchannel plate detector was variable. The laser intensity, extraction voltage, extraction delay time, lens voltage, and detector voltage were each varied in order to find the optimal instrument settings to measure the correct molecular mass distribution of the polymer mixture. The sample plate voltage and reflectron voltages were held constant because their numerical relationship is determined by the geometry of the ion optics system.

2.4. Sample preparation

Samples of each of the three polystyrenes was dissolved in unstabilized THF at a concentration of 5 mg mL⁻¹. These three solutions were mixed into a master solution corresponding to 70% *n*-butyl PS (GPC M_n 9030 u), 10% low mass *n*-octyl PS (GPC M_n 6100 u) and 20% high mass *n*-octyl PS (GPC M_n 12160 u). For each experiment fresh solutions of retinoic acid (50 mg mL⁻¹)

and AgTFA (5 mg mL⁻¹) were prepared in unstabilized THF. The choice of retinoic acid as the MALDI matrix was based in part on an interlaboratory comparison conducted by the National Institute of Standards and Technology (NIST) [13]. The polymer, matrix, and salt solutions were mixed in a ratio of 1:10:1 by mass. This solution was deposited onto the sample target by electrospray (ES) to increase signal repeatability by creating a uniform sample [14–16]. The electrospraying was done using a voltage of 5 kV and a flow rate of 5 μL min⁻¹. The sample target was held 3.8 cm from the tip of the needle. The sample target was divided in half by using Teflon film to mask one side at a time. The first side was electrosprayed with matrix and salt only (no polymer). This half of the target was used to create a background spectrum used later during the data analysis. Reversing the film position, the second side was electrosprayed with the polymer, matrix, and salt solution. In this way analyte spectra as well as background spectra could be taken on the same target at (nearly) the same time. This prevented temporal changes in the instrument stability from greatly affecting the measurement.

2.5. Instrument operation

The laser energy was tested both before and after the experiments to control for laser energy drift. This was done using a Laser Probe, Inc. (Utica, NY) model RM-3700 universal radiometer with a model RJP-465 silicon energy probe with a neutral density filter to bring the laser intensity to the middle of the detector's operating range. Averages of 20 laser shots were used because shot to shot variability is high for nitrogen gas lasers.

Rough calibration of the mass axis of the mass spectrometer was performed using a mixture of angiotensin II (1046.54 u), bovine insulin (5734.51 u) and cytochrome C (12 361.96 u). The rough calibration was improved by using five polymer peaks of known mass, three in the central *n*-butyl PS distribution and one each in the two *n*-octyl PS distributions.

2.6. Data collection

Several experiments could be completed in 1 day's time. An experiment consisted of five repeat spectra on the analyte side of the target and five repeat spectra on the blank side of the target for a total of 10 spectra. Each spectrum consisted of 1000 laser shots. This sequence was repeated for all five adjustable parameters (detector voltage, laser energy, delay time, extraction voltage and lens voltage). Each was varied from its initial setting (and then restored to its initial setting after spectrum collection) in random order. We found it necessary to recalibrate the mass axis after changing each of the following parameters: delay time, extraction voltage, and lens voltage.

Each iteration over the optimization loop produced 60 spectra: 30 for the analyte paired with 30 for the background. There are 30 for each because 5 instrument parameters are changed plus a set of spectra taken with no settings changed for a total of 6 possible instrument settings. There are 5 repeats at each setting giving us 6 × 5 = 30 spectra. Summing spectra for the analyte and the foreground there are 30 + 30 = 60 total spectra per optimization loop.

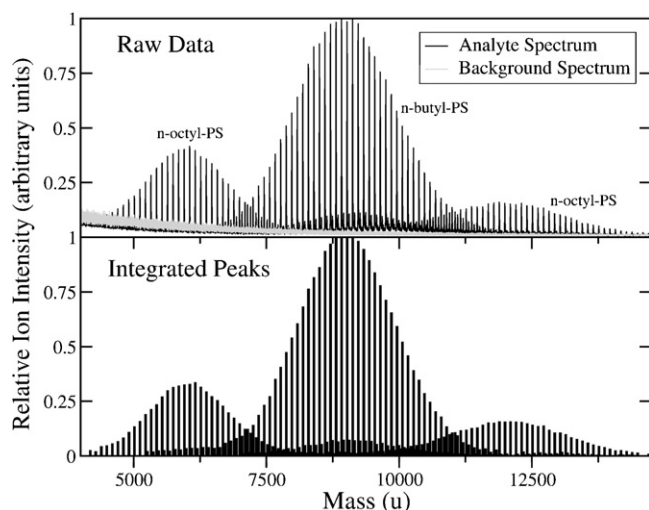


Fig. 1 – MALDI-TOF mass spectra of the mixture of three narrow-polydispersity polystyrenes. Top panel: analyte spectrum (black) and background spectrum (grey). Bottom panel: integrated analyte peak intensities using *MassSpectator* computer code [17–19].

2.7. Data analysis

The peaks in each spectrum were automatically identified and integrated using our *MassSpectator* software [17–19]. Additional code was written to take the peak positions with associated integrated peak areas provided by *MassSpectator* and, for each of the three polymers in the mixture, obtain a number proportional to the total measured mass attributable to each series and determine the moments of the molecular mass distribution for each series. This was done by sorting the individual peaks by mass into their corresponding series. The code also had the ability to recalibrate the mass axis using the largest peaks in the center of the molecular mass distribution.

The top panel of Fig. 1 shows a typical mass spectrum for the gravimetric mixture of the three polymers. In black is the analyte mass spectrum and overlaid in grey is the background spectrum. The background spectrum is taken with all the same conditions as the analyte spectrum except that the analyte is omitted from the target. The bottom panel of Fig. 1 shows the integrated peak intensities. Three polymer distributions are clearly visible. It can be seen that the different end group masses allow each peak to be sorted into its proper distribution with no ambiguity.

3. Numerical methods

The objective function used for the numerical optimization of the instrument parameters was:

$$J(x) = \left(\left(\frac{\sum_{MS}^{OPSL}}{\sum_{MS}^{BPS}} \right) - \left(\frac{OPSL_G}{BPS_G} \right) \right)^2 + \left(\left(\frac{\sum_{MS}^{OPSH}}{\sum_{MS}^{BPS}} \right) - \left(\frac{OPSH_G}{BPS_G} \right) \right)^2 \quad (1)$$

where OPSL and OPSH, represent the peaks in the spectrum associated with the low-mass and high-mass *n*-octyl-initiated polystyrenes, respectively. Likewise, BPS represents the *n*-butyl-initiated polystyrene. The summation Σ is over all the mass spectral peaks. The subscript G represents the gravimetric amounts of each polymer in the mixture. The variable x represents the five-dimensional vector of instrument settings. When $J(x)=0$ the integrated mass spectral peak ratios equal the gravimetric ratios and the instrument settings are at their optimum values.

The function $J(x)$ is a noisy function with respect to the parameter vector x due to the inherent statistical noise in the mass spectra. This complicates the task of numerically locating the minimum of $J(x)$. The fact that each evaluation of $J(x)$ requires an experiment, and subsequent interpretation of experimental results, means that there is a high cost for each function evaluation. This limits the number of function evaluations that are feasible and further complicates any numerical procedure that seeks to minimize $J(x)$. Taken together these factors make the task of finding a useful minimum of $J(x)$ a natural candidate for popular sampling optimization methods like genetic algorithms [20], simulated annealing algorithms [21], and direct search methods [22]. However, these methods are not the best available for a number of reasons. First, the large number of function evaluations required precludes their use in a reasonable way when the experiments are time consuming. Second, when the number of function evaluations grows too large it jeopardizes the physical assumptions on the continuity of $J(x)$ with respect to the vector x because as time passes a natural experimental irreproducibility occurs which arises primarily from instrument stability considerations. Third, all three of these algorithms may generate sample or trial points that cannot be evaluated, for example, out-of-range instrument parameter settings. Fourth, for these types of approaches the problem of terminating the minimization process is not well defined. This is especially true for an objective function whose output depends on a spectroscopic experiment where noise can be a significant factor.

One method for minimizing noisy functions that seeks to approximate the gradient of the objective function $\nabla J(x)$ is called *implicit filtering* [23]. Broadly speaking this method uses a very coarse grained step-length to build a finite-difference approximation to $\nabla J(x)$. This gradient is then used to generate steep-descent directions for a minimization process. As iterates draw closer to the solution, and the objective function decreases, the finite difference step-length is decreased until it approaches a number small enough to suggest convergence of the algorithm to the minimum value. The algorithm can be described qualitatively as follows:

- (1) Given x_0 , an initial set of instrument parameters.
- (2) Estimate noise in $J(x)$ with respect to each x_i .
- (3) Use the result of (2) to estimate, ε_i , the new step length.

- (4) Approximate the finite-difference gradient $\nabla J(x)$ using finite difference step-length.
- (5) Generate gradient-based search direction and apply to next iteration.
- (6) Check for convergence using the norm of the gradient and total change in parameter values.

Here the initial guess at the instrument parameter values, and the initial guess at the perturbation values ε_i , was generated by past experience with the instrument from a previous interlaboratory comparison on a similar polystyrene [13]. The estimate of the noise function is then used to find the value of the finite-difference step length parameter that maximized the expected value of the correct gradient. This probabilistic optimization maximizes the likelihood of the gradient being correct. This approach results in a gradient that can be used to generate a minimization search direction. In this experiment we used a Broyden–Fletcher–Goldfarb–Shanno (BFGS) method [8,24]; however, other gradient based methods to determine the search direction could have been employed. Finally, gradient-based convergence is used as the stopping criterion.

The method implemented here was motivated by the implicit filtering algorithm; however, the choice of the finite-difference step-length is based on a problem-specific estimation of the amount of noise in the objective function. In so doing, the algorithm will build an approximation to the gradient that perturbs in an amount proportional to the noise in the function. If one has a reasonable estimate of the noise in the function $J(x)$, this method has considerable benefits. It allows for a more rapid convergence than sampling methods that do not estimate the gradient, the gradient approximation can be used to yield information about the optimal parameters (for example confidence intervals) and finally this method attempts to collect data (or sample) in a region that appears to be more likely, probabilistically, to contain the solution. This *response surface methodology* (RSM) can also help determine if the norm of the gradient is sufficiently small to indicate convergence of the algorithm.

A few additional notes on this method bear mentioning. Constraints can be handled in a straightforward way by forming the appropriate Lagrangian function. In the case study described here the constraints did not become active, nor were they binding at the solution, thus we did not complicate the algorithm with details of Lagrange multiplier estimates. The algorithm appeared to converge to a reasonable prescribed tolerance after five iterations. The trajectory of convergence suggested that the gradient approximation was successful and that the noise in the objective function with respect to the parameter values, x , decreased with iterations. Both statistical sampling and RSM strongly indicated that the algorithm terminated at an optimum set of instrument parameters.

4. Results

Fig. 2 shows the objective function $J(x)$ and the value of its local gradient $\nabla J(x)$ as a function of iteration step. There is an initial steep drop in the objective function followed by gradual movement to the optimal parameter settings. The

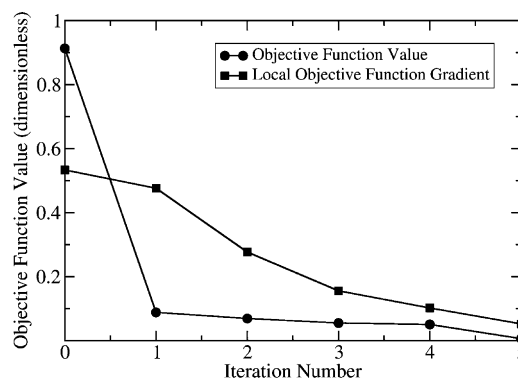


Fig. 2 – Value of the objective function $J(x)$ and its gradient $\nabla J(x)$ vs. iteration number. The zeroth iteration is the starting value.

gradient of the objective function also decreases steadily as the optimum point is approached. Similarly the step length in five-dimensional parameter space is also decreasing. These monotonic responses indicate that the optimization routine is converging robustly. At the optimum value the objective function is so small that it cannot be reduced further due to the inherent noise in the measurement. Likewise, the step size indicated for each parameter at this point is so small as to be below the precision of the instrument's settings. By this measure, the solution was clearly attained.

Fig. 3 shows the individual instrument parameter values as a function of iteration number. The uncertainties for the final (optimal) values are given in Table 1. (How the uncertain-

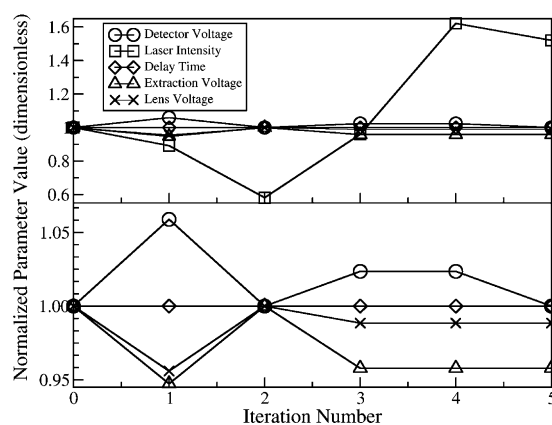


Fig. 3 – Instrument parameter value vs. iteration number. The zeroth iteration is the starting value.

Table 1 – Optimal instrument settings and confidence intervals at the 95% level

Instrument parameter	Optimal setting \pm confidence interval
Detector voltage	(1.7 \pm 0.03) kV
Laser intensity	(1.86 \pm 0.11) μ J/pulse
Delay time	500 ns
Extraction voltage	(18.2 \pm 0.80) kV
Lens voltage	(8.6 \pm 2.0) kV

ties were determined is described in the Section 5.) The values oscillate about their final values as the optimization proceeds. The laser intensity undergoes the greatest excursions decreasing in the first two iterations, returning to its initial value in the third iteration, and then increasing in the fourth iteration before settling into its final value. The four other parameters make an excursion in the direction of their final values in the first iteration, return to their initial value in the second iteration, and find the equilibrium values by the third iteration. This initial zigzag pattern is characteristic of gradient steps being applied to optimization a nonlinear function. This nonlinearity arises in the instrument parameters coupling, that is, varying one parameter requires all others to vary in a nonlinear response if $J(x)$ is to move closer to its optimal value. Thus, the vector x_{i+1} has a tendency to be normal to the vector x_i (in its five-dimensional space). The laser intensity varies the greatest amount and would seem to be the most sensitive variable. The primacy of the laser power setting is in accord with most users' experiences with MALDI-TOF mass spectrometry of synthetic polymers.

5. Discussion

Calculation of the confidence interval for each instrument parameter is critical in determining the Type B ("systematic") uncertainty in the measurement of the polymer MMD. To do this we employ a *profile-likelihood function* derived from the estimate of the derivatives of the objective function with respect to the variables over which we are optimizing. Caution must be exercised because we only have a secant approximation to first derivatives, that is, finite difference estimates with a coarse finite difference step-length parameter, and a weak (quasi-Newton) approximation to the matrix of second derivatives. The profile likelihood function used was the logarithmic-likelihood function [25]. This functional form was chosen over the more typically used Gaussian distribution because while the noise in the background spectra was Gaussian the noise in the analyte spectra had additional components that could not be modeled by a Gaussian distribution. Expressed another way, while the noise in the background spectra was indicative of the sum of many factors, the noise in the analyte spectra displayed noise that was the result of a multiplicative mechanism acting on some (or all) of these factors [26].

Now consider our solution, $x^* = (x_1^*, x_2^* \dots x_5^*)$, the optimized instrument parameters. Further consider the logarithmic distribution function, L , associated with the equation $x = x_i^*$ where x_i^* is our proposed optimal value of x_i ,

$$\begin{aligned} L_i^*(x_i^*) &= \max_x L(x) \\ \text{s.t. } x_i &= x_i^* \end{aligned} \quad (2)$$

If we take L^* to denote the logarithmic likelihood evaluated at the optimal value, $x_i = x_i^*$ then from elementary statistics $2(L^* - L_i^*(x_i^*))$ has a limiting χ^2 -distribution with a single degree of freedom [25]. Thus, a single degree of freedom $100(1-\alpha)$ percentile of the χ^2 -distribution, $(\chi_{1-\alpha,1}^2)^2$, obeys:

$$\chi_{1-\alpha,1}^2 = L^* - L \quad (3)$$

For x_i^* such that $L_i^*(x_i^*) \leq L$. The estimate $\nabla J(x)$ can be used to in conjunction with the approximate Hessian matrix (using the BFGS formulas). With a gradient and a reasonable Hessian approximation the sequential quadratic programming method can be used to solve numerically the constrained optimization problem (2) for the endpoints of the confidence intervals. Clearly any constrained nonlinear optimization algorithm could be employed. Using this method the list of parameters and confidence intervals at the 95% level for the optimal instrument settings are given in Table 1. Of course, with the ion-extraction delay time no uncertainty is possible since this is a discrete variable. We can only say with 95% confidence that the value is 500 ns and not the other two options, 250 ns and 750 ns.

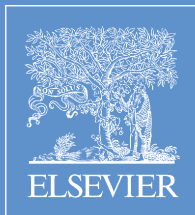
6. Conclusion

A specialized noise-adapted filtering method has been applied to the problem of finding the optimal instrument parameters for a MALDI-TOF mass spectrometer. Finding the optimal instrument parameters was a critical step in creating an absolute molecular mass distribution polymer Standard Reference Material. The task of tuning the instrument's five main parameters could not be approached by exhaustive search methods given the amount of effort needed to take and to reduce the data in a statistically meaningful way at each set of instrument parameters. Additionally, this method produces an estimate of the sensitivity of each optimal parameter estimate not available to traditional exhaustive search methods. Each of the subtasks in the process could be automated to create an integrated closed-loop optimization scheme.

REFERENCES

- [1] K. Tanaka, H. Waki, Y. Ido, S. Akita, Y. Yoshida, T. Yoshida, *Rapid Commun. Mass Spectrom.* 2 (1988) 151–153.
- [2] J.A. Castro, C. Köster, C.L. Wilkins, *Rapid Commun. Mass Spectrom.* 6 (1992) 239–241.
- [3] U. Bahr, A. Deppe, M. Karas, F. Hillenkamp, *Anal. Chem.* 64 (1992) 2866–2869.
- [4] C.N. McEwen, C. Jackson, B.S. Larsen, *Int. J. Mass Spectrom. Ion Processes* 160 (1997) 387–394.
- [5] D. Vitalini, P. Mineo, E. Scamporrino, *Rapid Commun. Mass Spectrom.* 13 (1999) 2511–2517.
- [6] S.J. Wetzel, C.M. Guttman, K.M. Flynn, J.J. Filliben, *J. Am. Soc. Mass Spectrom.* 17 (2006) 246–252.
- [7] D.P. Bertsekas, *Nonlinear Programming*, Athena Scientific, Belmont, MA, 1999.
- [8] C.T. Kelley, *Iterative Methods for Optimization*, Society for Industrial and Applied Mathematics, Philadelphia, 1999.
- [9] J.C. Spall, *Introduction to Stochastic Search and Optimization*, Wiley-Interscience, Hoboken, NJ, 2003.
- [10] S. Vaidyanathan, D.I. Broadhurst, D.B. Kell, R. Goodacre, *Anal. Chem.* 75 (2003) 6679–6686.
- [11] S. O'Hagan, W.B. Dunn, M. Brown, J.D. Knowles, D.B. Kell, *Anal. Chem.* 77 (2005) 290–303.
- [12] Certain equipment, instruments or materials are identified in this paper in order to adequately specify the experimental details. Such identification does not imply recommendation by the National Institute of Standards and Technology nor does it imply the materials are necessarily the best available for the purpose.

- [13] C.M. Guttman, S.J. Wetzel, W.R. Blair, B.M. Fanconi, J.E. Girard, R.J. Goldschmidt, W.E. Wallace, D.L. VanderHart, *Anal. Chem.* 73 (2001) 1252–1262.
- [14] J. Axelsson, A.M. Hoberg, C. Waterson, P. Myatt, G.L. Shield, J. Varney, D.M. Haddleton, P.J. Derrick, *Rapid Commun. Mass Spectrom.* 11 (1997) 209–213.
- [15] R.R. Hensel, R.C. King, K.G. Owens, *Rapid Commun. Mass Spectrom.* 11 (1997) 1785–1793.
- [16] S.D. Hanton, I.Z. Hyder, J.R. Stets, K.G. Owens, W.R. Blair, C.M. Guttman, A.A. Giuseppetti, *J. Am. Soc. Mass Spectrom.* 15 (2004) 168–179.
- [17] W.E. Wallace, A.J. Kearsley, C.M. Guttman, *Anal. Chem.* 76 (2004) 2446–2452.
- [18] A.J. Kearsley, W.E. Wallace, C.M. Guttman, *Appl. Math. Lett.* 18 (2005) 1412–1417.
- [19] A.J. Kearsley, *J. Res. Natl. Inst. Stand. Technol.* 111 (2006) 121–125.
- [20] D.E. Goldberg, *Genetic Algorithms in Search, Optimization, and Machine Learning*, Addison-Wesley, Reading, MA, 1989.
- [21] S. Kirkpatrick, C.D. Gelatt Jr., M.P. Vecchi, *Science* 220 (1983) 671–680.
- [22] T.G. Kolda, R.M. Lewis, V. Torczon, *SIAM Rev.* 45 (2003) 385–482.
- [23] P. Gilmore, C.T. Kelley, *SIAM J. Optim.* 5 (1995) 269–285.
- [24] J. Nocedal, S.J. Wright, *Numerical Optimization*, Springer-Verlag, New York, 1999.
- [25] R.V. Hogg, A.T. Craig, *Introduction to Mathematical Statistics*, MacMillan, New York, 1978.
- [26] J.R. Benjamin, C.A. Cornell, *Probability, Statistics, and Decision for Civil Engineers*, McGraw Hill, New York, 1970.



ANALYTICA CHIMICA ACTA

AN INTERNATIONAL JOURNAL DEVOTED TO ALL BRANCHES OF ANALYTICAL CHEMISTRY

Editors:

Richard P. Baldwin
Lutgarde Buydens
Purnendu K. Dasgupta
Ulrich J. Krull
Hian Kee Lee
Liang Li
Janusz Pawliszyn
Alan Townshend
Paul J. Worsfold

Review Editor:

Manuel Miró

SPECIAL ISSUE

Papers presented at the 3rd INTERNATIONAL SYMPOSIUM
ON THE SEPARATION AND CHARACTERIZATION OF
NATURAL AND SYNTHETIC MACROMOLECULES

Amsterdam, The Netherlands

31 January–2 February 2007

Edited by: Peter Schoenmakers and Robert Smits